

This discussion paper is/has been under review for the journal Hydrology and Earth System Sciences (HESS). Please refer to the corresponding final paper in HESS if available.

# Turbulent flux modelling with a simple 2-layer soil model and extrapolated surface temperature applied at Nam Co Lake basin on the Tibetan Plateau

T. Gerken<sup>1,2</sup>, W. Babel<sup>2</sup>, A. Hoffmann<sup>1</sup>, T. Biermann<sup>2</sup>, M. Herzog<sup>1</sup>, A. D. Friend<sup>3</sup>, M. Li<sup>4</sup>, Y. Ma<sup>5</sup>, T. Foken<sup>2</sup>, and H.-F. Graf<sup>1</sup>

<sup>1</sup>Centre for Atmospheric Science, Department of Geography, University of Cambridge, UK

<sup>2</sup>Department of Micrometeorology, University of Bayreuth, Germany

<sup>3</sup>Department of Geography, University of Cambridge, UK

<sup>4</sup>Cold and Arid Region Environmental and Engineering Research Institute, Chinese Academy of Sciences, Lanzhou, China

<sup>5</sup>Institute of Tibetan Plateau Research, Chinese Academy of Sciences, Beijing, China

Received: 19 October 2011 – Accepted: 31 October 2011 – Published: 21 November 2011

Correspondence to: T. Gerken (tobias.gerken@uni-bayreuth.de)

Published by Copernicus Publications on behalf of the European Geosciences Union.

10275

## Abstract

This paper introduces a surface model with two soil-layers for use in a high-resolution circulation model that has been modified with an extrapolated surface temperature, to be used for the calculation of turbulent fluxes. A quadratic temperature profile based on the layer mean and base temperature is assumed in each layer and extended to the surface. The model is tested at two sites on the Tibetan Plateau near Nam Co Lake during four days during the 2009 Monsoon season. In comparison to a two-layer model without explicit surface temperature estimate, there is a greatly reduced delay in diurnal flux cycles and the modelled surface temperature is much closer to observations. Comparison with a SVAT model and eddy covariance measurements shows an overall reasonable model performance based on RMSD and cross correlation comparisons between the modified and original model. A potential limitation of the model is the need for careful initialisation of the initial soil temperature profile, that requires field measurements. We show that the modified model is capable of reproducing fluxes of similar magnitudes and dynamics as the more complex methods chosen as reference.

## 1 Introduction

Turbulent fluxes of momentum, latent and sensible heat are some of the most important interactions between land surface and atmosphere. These fluxes are responsible for the development or modification of mesoscale circulations and the generation of clouds that, as a consequence, feed back on surface fluxes through the modification of solar radiation. The effects of vegetation influencing boundary layer structure and moisture are widely acknowledged (i.e. Freedman et al., 2001; van Heerwaarden et al., 2009), while the feedback from short-lived clouds is less understood, but important. Shallow cumulus-surface interactions were shown in an LES study to impact surface temperature and fluxes on very short time scales (Lohou and Patton, 2011). For improved process understanding, it is necessary to use: (1) atmospheric models with sufficiently

10276

high resolution to resolve boundary layer processes as well as clouds and (2) surface models capable of reproducing the system's surface flux dynamics.

Our research focuses on surface-atmosphere interactions on the Tibetan Plateau (TP) in the Nam Co Lake region. With more than 4700 m a.s.l., a semi-arid climate and with a highly adapted *Kobresia pygmaea* alpine steppe (Miehe et al., 2011), the TP proves to be a difficult environment for surface models (Yang et al., 2003, 2009). Specific problems include large temporal and spatial variability in soil moisture (Su et al., 2011), large diurnal variations of surface temperature from surface freezing before sunrise to more than 30 °C at noon. Ma et al. (2009) give an overview about the TP surface-atmosphere processes. On the TP, the fraction of diffuse solar radiation is very small, making cloud feedbacks especially important for the surface-atmosphere system. The model studies with a regional model of Cui et al. (2007) imply that some of the precipitation events on the TP are predominantly local and therefore not captured by coarser resolution models.

In this paper we present results of a rather simple two-layer flux algorithm based on a two-layer soil model that is part of a vegetation dynamics and biosphere model (Friend, 2010). The original model produces a substantial delay in the diurnal turbulent flux cycle due to the low responsiveness of the upper model layer to changes in atmospheric forcing and fails to capture important dynamics. We therefore introduce an extrapolated surface temperature and show that this is capable of reproducing diurnal flux dynamics for two vegetation covered surfaces near Nam Co Lake. These sites are representative for the basin, but show very different dynamics. In our future studies, the same surface-model version will also be coupled to a spatially and temporally high resolution atmospheric model including radiation, cloud microphysics and active tracer transport. As simulations of the high-resolution model will be run for approximately 24 h we tested the surface model in column mode forced with standard atmospheric measurements for the same period of time with initialisation at 00:00 h Beijing Standard Time (BST). We acknowledge that this approach is different from most surface model studies that are run for longer periods, but it is necessary for the planned study

10277

of the coupled surface-atmosphere system. Such a surface flux algorithm is generally suitable for high-resolution atmospheric modelling studies of different ecosystems as it does not have built in assumptions about horizontal scales.

It is our objective to test the suitability of a simple two-layer soil model with an improved surface or “skin” temperature estimated from the mean temperature of the uppermost layer that shall subsequently be used for driving an atmospheric circulation model for the Nam Co region on the TP. Therefore, fluxes derived from the surface flux algorithm with and without a specific formulation for “skin” temperature are compared to measured fluxes by eddy covariance technique and to fluxes derived by a more complex Soil-Vegetation-Atmosphere Transport (SVAT) Model, with five soil layers.

## 2 Site description and experimental data

Nam Co Lake is located on the Tibetan Plateau at approximately 4730 m a.s.l., circa 150 km north of Lhasa. During the monsoon season of 2009 a joint measurement campaign was conducted from 27 June to 8 August by the University of Bayreuth (UBT) and the Institute of Tibetan Plateau Research – Chinese Academy of Sciences (ITP). Data from 2 locations are used. Site 1, both referred to and operated by UBT is an eddy covariance complex close to the shore of a small lake next to Nam Co lake. UBT has a fairly constant soil moisture below circa 60 cm depth due to the influence of a water table. Additionally, the atmospheric measurements are influenced by a land lake breeze. Site 2 (operated by and referred to as ITP) is at the Nam Co Station for Multisphere Observation and Research (Li et al., 2009; Cong et al., 2009), approximately 300 m distant from both UBT and the lake with a sandy soil and a very low field capacity (FC = 5 %) compared to overall pore volume (39 %). The vegetation at both sites is grassland (Metzger et al., 2006) with UBT having a small bare soil fraction (0.1) compared to 0.4 at ITP). Small FC and the generally low volumetric top soil water contents ( $\theta_v$ ) at ITP, lead to large sensible energy fluxes compared to latent heat fluxes ( $Q_H \gg Q_E$ ). After rain events however,  $\theta_v$  may exceed FC by a factor of up to 3 leading

10278

to a similar flux regime at the two stations with  $Q_E > Q_H$ . Due to the generally drier conditions at ITP, surface temperature frequently drops below  $0^\circ\text{C}$  in the early morning hours. At UBT there were soil temperature sensors installed at 2.5, 5, 10, 20, 30 and 50 cm depths. At ITP no accurate soil temperatures were available at depths less than 20 cm. Comprehensive information of ITP and UBT surface and soil properties is found in Table 1.

## 2.1 Forcing data

The 24-h model runs are initialised with the soil temperature profile and soil moisture at 00:00 h BST ( $\sim 22:00$  in local solar time). Four days were selected from the campaign representing different weather conditions. 10 July was a complex day with rain in the morning and sunshine in the afternoon. 27 July was a cloudy day without rain. 5 August was a radiation day after a period of rain leading to moist conditions and large  $Q_E$  at ITP. 6 August was similar to the previous day, but with some of the water drained from the soil at ITP and developing clouds in the afternoon. During 10 July and 5 August, the station close to the lake (UBT) came under the influence of a lake breeze during which the forcing data (except for radiation measurements) correspond rather to the nearby lake than the land surface. Due to the overcast sky on 27 July the lake breeze was severely weakened as described in Zhou et al. (2011), so that there was only limited influence of the lake surface onto the atmospheric measurements.

The model is forced with measured atmospheric data from two sites on the TP providing air temperature, water vapour mixing ratio, wind speed, air pressure, precipitation and downwelling long and shortwave radiation. These data are displayed in Fig. 1 for UBT and Fig. 2 for ITP. In general 30-min mean values were linearly interpolated to the surface model time step that was the same as a typical time step of an atmospheric model ( $\Delta t = 2.5$  s). The only selected day with precipitation (rain) during day-time was 10 July 2009. However, there was also rain recorded at UBT from about 22:00 h BST on 6 August 2009. Half hourly precipitation was scaled down to the model time step assuming a constant precipitation rate per 30-min interval. There was little difference

10279

between the data measured at ITP and UBT, as expected due to the proximity of the sites. However there was an offset of approx. 5 hPa between the recorded pressures, that was not corrected for as this is likely within the uncertainty of the sensors and the model should not be too sensitive to such a pressure difference. Unlike UBT where rain 30-min precipitation was available, there were only daily sums recorded for ITP, which had to be downscaled to 30-min values by scaling them linearly with UBT observations.

## 3 Modelling approach

The surface model Hybrid (Friend et al., 1997; Friend and Kiang, 2005) is currently coupled to the high-resolution Active Tracer High-resolution Atmospheric Model (ATHAM) by Oberhuber et al. (1998) and Herzog et al. (1998) for the investigation of feed-backs between atmospheric processes and surface fluxes.

Our high-resolution modelling approach aims at a spatial and temporal resolution in the order of 500 m and 2.5 s, respectively. As our focus is on diurnal surface-atmosphere interactions, the surface model must capture the magnitude of the fluxes and must be able to react quickly to changes in atmospheric forcing. Therefore, a surface model that is capable of reproducing realistic turbulent energy and water vapour fluxes at a sufficiently high temporal resolution and at reasonable computational costs is needed. We decided against a model with more than two soil-layers due to higher computational cost and instead modified the original Hybrid model to meet these requirements.

### 3.1 The surface model

The modified version of Hybrid which is a process based terrestrial ecosystem and surface model, incorporates a simple two-layer representation of the soil and uses the turbulent transfer parameterisations taken from the GISS model II (Hansen et al., 1983). The transfer equations in Hybrid are described in Friend and Kiang (2005). Bare

soil parameterisation follows the approach of SSiB (Xue et al., 1996) that is based on Camillo and Gurney (1986) and Sellers et al. (1986). Turbulent fluxes are calculated using a bulk approach for the sensible heat flux ( $Q_H$ ):

$$Q_H = c_p \rho C_H u(z) (T_0 - T(z)) \quad (1)$$

5 with air specific heat capacity ( $c_p$  [ $\text{Jkg}^{-1}\text{K}^{-1}$ ]), the Stanton number ( $C_H$ ) which is calculated as a function of roughness length  $z_0$  and Bulk Richardson Number, air density ( $\rho$  [ $\text{kgm}^{-3}$ ]), measured wind speed ( $u(z)$  [ $\text{ms}^{-1}$ ]) and air temperature ( $T(z)$ ) at measurement height  $z$  [m] and with  $T_0$  being the surface temperature. All temperatures used are in K. The latent heat flux ( $Q_E$ ) is derived in a more complex manner from bulk soil  
10 evaporation and a canopy resistance approach estimating plant transpiration. Transfer coefficients are modified from Deardorff (1968). Plant physiology and stomatal conductance are included via generalised plant types (GPT). As an ecosystem model Hybrid is designed to work on hourly to climate scales (Friend, 2010) and should therefore be capable of reproducing diurnal flux cycles as well as ecosystem changes on climate  
15 scales. It was originally developed as a biosphere-surface component for the GISS GCM. A “thin” upper layer with 10 cm thickness follows the daily cycle of surface temperatures, whereas a lower layer with 4 m thickness acts as the memory for the annual cycle. However, an upper layer of such thickness imposes a substantial dampening on the diurnal temperature cycle and will effectively act as a lowpass filter for events  
20 of short durations such as cloud shading that, especially under the conditions found at the TP, has a substantial immediate impact on surface temperatures and on fluxes as well. This is also seen in Fig. 12 of Hansen et al. (1983), where a time delay of approximately 2 h is visible for surface temperature in the diurnal cycle. A similar behaviour of the original Hybrid is discussed in Sect. 5.4. Shortcomings with the representation of  
25 diurnal cycles may also impact on longer term studies as the model drifts away from a realistic state. As we plan to apply the coupled model for high-resolution simulations with a time step in the order of seconds, we focus in this work on the accuracy of the diurnal flux cycles that can be achieved with such a model.

10281

### 3.2 The modified soil model in Hybrid

Two main changes that lead to a better representation of the actual soil state have been introduced to Hybrid. They address its main problems of a delay in diurnal flux evolution and its weak responsiveness to sudden short-term changes in atmospheric  
5 forcing.

#### 3.2.1 Diagnostic surface temperature

An extrapolated surface temperature ( $T_0$ ) is being introduced that is then subsequently used for the calculation of atmospheric stability through the Bulk Richardson number as well as for  $Q_H$  and  $Q_E$ . This approach is somewhat similar to the “force-restore  
10 method” (Blackadar, 1979) that also aims at providing a realistic surface temperature imitating the behaviour of real soils. However, while “force-restore” uses an oscillating heat source as forcing term and a heat-flux into the ground as restoring term (Yee, 1988), our method is not dependent on a periodic heating function and uses the concept of layer heat storage.  $T_0$  is derived from a set of assumptions that were already  
15 included in Hybrid going back to Hansen et al. (1983). For both layers denoted with the subscripts 1 and 2 from the model top, we assume a quadratic temperature profile  $T(z)$  (Fig. 3):

$$T_{1,2}(z_{\text{rel}}) = a_{1,2} (z_{\text{rel}} - d_{1,2})^2 + T_{\text{base}_{1,2}} \quad (2)$$

with  $a$  [ $\text{Km}^{-2}$ ] being a constant,  $z_{\text{rel}}$  [m] the depth below the top of the layer,  $d$  [m] the  
20 layer thickness and  $T_{\text{base}}$  as temperature at the base of the respective layers. There is no transfer of heat through the lower boundary of the model so that  $T_{\text{base}_2}$  is constant and equal to annual mean temperature. The relationship between layer heat content  $E$  [J] and temperature profile is given by:

$$E = c_p \int_{z_L}^{z_U} T(z) dz \quad (3)$$

10282



Table 2 shows the initial temperatures for each day. From the span of layer temperatures  $\bar{T}_1$  and  $\bar{T}_2$ , the theoretical parameter space of  $T_0$  for a constant  $T_{\text{base}_2}$  (Fig. 4) can be derived. A random combination of the initial temperatures given in Table 2 would yield  $T_0$  in the range of  $-10$  to  $30^\circ\text{C}$ . In contrast, the actual model layer temperatures, indicated by the crosses in Fig. 4c, occupy a much smaller area and are, with the exception of one day, clustered closely. This highlights the importance of a careful initialisation of the soil temperature profile requiring knowledge about subsurface temperatures that are difficult to estimate without field measurements.

#### 4 Flux comparison

Surface fluxes derived with any method contain inaccuracies such as measurement errors or theoretical limitations. Therefore we are not comparing our modelling results to the absolute truth, but to two flux references.

##### 4.1 EC and SEWAB reference fluxes

Fluxes estimated by both versions of Hybrid are compared with observed fluxes derived by eddy covariance (EC) method and fluxes modeled by the SVAT model SEWAB (Surface Energy and Water Balance model – Mengelkamp et al., 1999), which has been calibrated to the two sites for gap-filling and up-scaling of flux measurements. Both flux references yield fluxes averaged over 30-min intervals. Unlike many SVAT models that derive the soil heat flux from the flux residual, SEWAB is solving the surface energy balance equation ( $Q_E + Q_H + Q_{\text{Rad}} + Q_{\text{Soil}} = 0$ ) iteratively for  $T_0$  by Brent's method (Mengelkamp et al., 1999), hence closing the energy balance locally (Kracher et al., 2009). In contrast, the surface energy balance closure derived by EC is only in the order of 0.7 at Nam Co Lake (Zhou et al., 2011). This means that 30% of the net radiation is not captured by surface flux measurements. However, energy balance closure must not be used as a quality measure for flux measurements (Aubinet et al., 1999)

10285

as surface heterogeneity leads to organised low frequency structures and mesoscale circulations (Panin et al., 1998; Kanda et al., 2004) that are mainly responsible for the lack of closure (Foken, 2008). This is especially true for sea (lake) breeze systems, where a significant portion of the energy fluxes is transported horizontally (Kuwagata et al., 1994). Therefore, SEWAB (and Hybrid) fluxes are comparatively larger than measured ones. When the energy balance is closed artificially by redistributing the residual to fluxes according to the Bowen ratio (Twine et al., 2000), the resulting fluxes are in much better agreement with SEWAB (Babel et al., 2011). Therefore we use, when possible, energy balance corrected fluxes ( $Q_{E_{\text{EC,EBC}}}$  and  $Q_{H_{\text{EC,EBC}}}$ ). EC data were collected at 3 m height and calculated using the TK3 package (Mauder et al., 2008; Mauder and Foken, 2011). Quality checks were performed according to Foken et al. (2004). A detailed description of the instrumentation can be found in Biermann et al. (2009). The rain event of 10 July leads to the exclusion of fluxes due to quality concerns. Both Hybrid and SEWAB produce fluxes during rain, but their quality is unknown as they cannot be compared to measurements.

Measuring in close proximity to the lake also means that depending on wind direction the fluxes measured at UBT are originating from land, water or a mixture of both as the footprint of the EC system and the forcing data is located upwind of the site. This leads to problems in the energy balance closure and the integration of fluxes. The development of a lake breeze system at Nam Co means that during most days there are no flux measurements available from the late morning or early afternoon until the lake breeze ceases. The days of 27 July and 6 August are the only days during which the field campaign provides data that do not have a full lake breeze influence at UBT. Therefore it is beneficial to compare not only to measured fluxes, but also to SEWAB ( $Q_{E_{\text{SEWAB}}}$  and  $Q_{H_{\text{SEWAB}}}$ ).

For completeness, fluxes over the lake calculated by the TOGA-COARE algorithm (Fairall et al., 1996a,b) that is also part of the coupled surface-atmosphere model are given during lake breeze events.

10286

## 4.2 Statistical evaluation measures

In order to assess the model quality we use Root Mean Square Deviation (RMSD) and Cross Correlation (Eq. 11):

$$\text{RMSD} = \sqrt{\frac{1}{N} \sum_{i=1}^N (P_p - P_r)_i^2} \quad (10)$$

$$R^2(j) = \left( \frac{\text{cov}(P_p(1+j:N), P_r(1:N-j))}{\sigma_{P_p(1+j:N)} \sigma_{P_r(1:N-j)}} \right)^2 \quad (11)$$

with  $R^2(j)$  being the coefficients of determination for the predicted ( $P_p$ ) and reference ( $P_r$ ) flux time series shifted by  $j$  elements, the total number of elements in each time series ( $N$ ) and  $\sigma$  as their respective standard deviations. Both SEWAB and EC measurements produce 30-min flux averages, whereas Hybrid was set to 10-min averaged fluxes. Therefore the reference fluxes were linearly interpolated to Hybrid's output times before statistical evaluation. Periods when no energy balance corrected EC measurements were available were excluded from the calculation of the statistical measures.

## 5 Results and discussion

The following section presents and discusses the improvements that are achieved for a simple two-layer model when the formulation for surface temperature is included.

The original two-layer model Hybrid fails to reproduce the diurnal dynamics observed at UBT due to the thermal inertia of the top-layer. The delayed response in surface temperature leads to a shift in the resulting turbulent surface fluxes. This causes an underestimation of  $Q_E$  and  $Q_H$  until  $\sim 18:00$  h BST and later to an overestimation due to delayed surface cooling. The improvement of the modified Hybrid over the original formulation is discussed in more detail in Sects. 5.1 and 5.4.

10287

The latent (Fig. 5 – left column) and sensible heat fluxes (right column) estimated with the modified Hybrid model are generally in good agreement with the reference fluxes derived by EC and SEWAB. The diagnostic surface temperature (right column) also shows a close agreement. In some instances there remains a small shift in fluxes compared to the reference values, but this has been greatly improved compared to the original Hybrid. The surface temperatures are also in good agreement after sunrise, despite the fact that during the clear sky days in August there is excessive night-time surface cooling simulated by model. This is less of an issue during the overcast nights.

The situation at ITP is quite similar to UBT. The modified model agrees well with the EC and SEWAB reference data. On 5 August the turbulent flux dynamics match the EC measurements closely (Fig. 6), while the original Hybrid showed a strong delay in the flux response as the soil remained frozen during the morning. The same is true for the magnitude of the latent heat flux, but not for  $Q_H$  where Hybrid produces fluxes of a similar magnitude as SEWAB. These are considerably larger than the fluxes measured by EC and corrected for energy balance closure. For 6 August the modelled maximum of  $Q_E$  is larger than the maximum  $Q_{E_{EC,EBC}}$  and much greater throughout most of the day compared to SEWAB.  $Q_H$  in contrast shows similar diurnal dynamics as  $Q_{H_{EC,EBC}}$ , but with its magnitude closer to the sensible heat flux derived by SEWAB. This starts to diverge around 18:00 h. A large negative  $Q_H$ -flux in the morning hours is apparent but greatly improved compared to the unmodified Hybrid version. Figure 5a and b also highlights some limitations of ecosystem research as a large portion of the data had to be rejected due to limitations described in Sect. 4.1.

During lake breeze events the surface fluxes over water derived from TOGA-COARE are displayed. Sensible heat fluxes are in close agreement with EC data and fluxes derived by a hydrodynamic multi-layer lake model (Foken, 1984; Panin et al., 2006). Latent heat fluxes show a similar behaviour and are of similar magnitude on 10 July and 6 August. On 5 August there is at least a qualitative agreement between COARE and EC measurements.







## 5.5 Natural variability of fluxes

Atmospheric quantities and turbulent surface fluxes have a large natural variability that is difficult to measure or to model. The EC approach is dependent on averaging procedures and most standard measurements will yield mean values. In order to use high-frequency measurements for flux estimation, less common techniques such as conditional sampling or wavelet-spectra have to be used. Even if models are capable of reproducing variability on realistic scales it is difficult to supply forcing data with similar resolution. The forcing data used in this study, sampled and averaged 10 or 30 min means, are used for SEWAB. Running Hybrid at time steps comparable to a high-resolution mesoscale model requires interpolation of the forcing data and therefore potentially causes a smoothing of the model's response compared to the actual weather forcing as it would be provided by a coupled model. As surface models share a similar approach to the parameterisation of surface fluxes and close the surface energy balance locally, SEWAB and Hybrid fluxes are more similar to each other than they are to field measurements.

## 6 Conclusions

The accurate generation of surface fluxes is a necessary pre-requisite for studies of surface-atmosphere interactions and local to mesoscale circulations. In order to gain a better process understanding of the interaction between atmospheric circulation, clouds, radiation and surface fluxes, the generated diurnal flux cycles have to be of realistic magnitude and without temporal shift. The original two-layer surface model without a specific formulation for  $T_0$  produced both a considerable time lag and failed to capture the full diurnal dynamics due to its unresponsiveness.

We have demonstrated that the introduction of an extrapolated surface temperature enables even a quite simplistic soil model to realistically estimate turbulent surface fluxes and skin temperatures. The delay of fluxes during the daily cycle was greatly

10293

reduced, making the model usable for diurnal process studies. The total magnitude of fluxes is also much improved, when few and computationally cheap additional physically based processes are introduced. Comparing SEWAB with Hybrid, the RMSD for both fluxes and surface temperature is decreased by generally 40–60%. The improvement in quality was somewhat more varied in comparison to EC measurements, as comparison of models and measurements is not straight forward. The improved  $R^2(j)$  for smaller values of  $j$  shows that temporal shifts of the flux time series have been greatly reduced and the overall correlations are high. As with any natural system it is impossible to obtain complete data sets that capture the full amount of natural variability. However, the modified model has been tested for a larger spectrum of environmental conditions on the TP and produced reasonable results for both dry and moist conditions.

We have shown that a rather simple soil surface model can efficiently calculate turbulent fluxes at a high temporal resolution when driven by realistic atmospheric conditions. Nevertheless, it is quite clear that such an approach with extrapolated surface temperature needs careful model initialisation. The initial soil heat contents and therefore knowledge of soil temperature profiles is necessary. Due to the fact that the surface temperature in this study is a purely diagnostic quantity, there may still be some limitations such as a delayed or smoothed response to atmospheric forcing on very short timescales, such as the feedback between passing boundary-layer clouds and the surface fluxes. The influence of surface fluxes and their dynamics to regional circulation will be investigated in a future study.

*Acknowledgements.* This research was funded by the German Research Foundation (DFG) Priority Programme 1372 ‘‘Tibetan Plateau: Formation, Climate, Ecosystems’’ as part of the Atmosphere – Ecology – Glaciology – Cluster (TiP-AEG). ITP data was provided through CEOP-AEGIS, which is a EU-FP7 Collaborative Project/ Small or medium-scale focused research project – Specific International Co-operation Action coordinated by the University of Strasbourg, France under the call ENV.2007.4.1.4.2: ‘‘Improving observing systems for water resource management.’’ The authors would like to thank everyone who has contributed to the collection of field data in one of the world’s most remote regions. ADF acknowledges

10294



- Weather Rev., 111, 609–662, 1983. 10280, 10281, 10282, 10283
- Herzog, M., Graf, H., Textor, C., and Oberhuber, J. M.: The effect of phase changes of water on the development of volcanic plumes, *J. Volcanol. Geoth. Res.*, 87, 55–74, doi:10.1016/S0377-0273(98)00100-0, 1998. 10280
- 5 Hu, Z., Yu, G., Fu, Y., Sun, X., Li, Y., Shi, P., Wang, Y., and Zheng, Z.: Effects of vegetation control on ecosystem water use efficiency within and among four grassland ecosystems in China, *Glob. Change Biol.*, 14, 1609–1619, doi:10.1111/j.1365-2486.2008.01582.x, 2008. 10291
- Kanda, M., Inagaki, A., Letzel, M. O., Raasch, S., and Watanabe, T.: LES Study of the Energy Imbalance Problem with Eddy Covariance Fluxes, *Bound.-Lay. Meteorol.*, 110, 381–404, doi:10.1023/B:BOUN.0000007225.45548.7a, 2004. 10286
- 10 Kracher, D., Mengelkamp, H., and Foken, T.: The residual of the energy balance closure and its influence on the results of three SVAT models, *Meteorolog. Z.*, 18, 647–661, doi:10.1127/0941-2948/2009/0412, 2009. 10285
- 15 Kuwagata, T., Kondo, J., and Sumioka, M.: Thermal effect of the sea breeze on the structure of the boundary layer and the heat budget over land, *Bound.-Lay. Meteorol.*, 67, 119–144, doi:10.1007/BF00705510, 1994. 10286
- Li, M., Ma, Y., Hu, Z., Ishikawa, H., and Oku, Y.: Snow distribution over the Namco lake area of the Tibetan Plateau, *Hydrol. Earth Syst. Sci.*, 13, 2023–2030, doi:10.5194/hess-13-2023-2009, 2009. 10278
- 20 Lohou, F. and Patton, E. G.: Land-surface response to shallow cumulus, EGU General Assembly, Vienna, Austria, 3–8 April 2011, EGU2011-10280-1, 2011. 10276
- Ma, Y., Wang, Y., Wu, R., Hu, Z., Yang, K., Li, M., Ma, W., Zhong, L., Sun, F., Chen, X., Zhu, Z., Wang, S., and Ishikawa, H.: Recent advances on the study of atmosphere-land interaction observations on the Tibetan Plateau, *Hydrol. Earth Syst. Sci.*, 13, 1103–1111, doi:10.5194/hess-13-1103-2009, 2009. 10277
- 25 Mauder, M. and Foken, T.: Documentation and instruction manual of the eddy covariance software package TK3, *Arbeitsergebnisse* 46, University of Bayreuth, ISSN 1614-8916, Bayreuth, 2011. 10286
- 30 Mauder, M., Oncley, S. P., Vogt, R., Weidinger, T., Ribeiro, L., Bernhofer, C., Foken, T., Kohsiek, W., Bruin, H. A. R., and Liu, H.: The energy balance experiment EBEX-2000. Part II: Inter-comparison of eddy-covariance sensors and post-field data processing methods, *Bound.-Lay. Meteorol.*, 123, 29–54, doi:10.1007/s10546-006-9139-4, 2006. 10290

10297

- Mauder, M., Desjardins, R. L., and MacPherson, I.: Scale analysis of airborne flux measurements over heterogeneous terrain in a boreal ecosystem, *J. Geophys. Res.*, 112, D13112, doi:10.1029/2006JD008133, 2007. 10290
- 5 Mauder, M., Foken, T., Clement, R., Elbers, J. A., Eugster, W., Grnwald, T., Heusinkveld, B., and Kolle, O.: Quality control of CarboEurope flux data - Part 2: Inter-comparison of eddy-covariance software, *Biogeosciences*, 5, 451–462, doi:10.5194/bg-5-451-2008, 2008. 10286
- Mengelkamp, H., Warrach, K., and Raschke, E.: SEWAB – a parameterization of the Surface Energy and Water Balance for atmospheric and hydrologic models, *Adv. Wat. Resour.*, 23, 165–175, doi:10.1016/S0309-1708(99)00020-2, 1999. 10285
- 10 Metzger, S., Ma, Y., Markkanen, T., Göckede, M., Li, M., and Foken, T.: Quality assessment of Tibetan Plateau Eddy Covariance measurements utilizing Footprint modeling, *Adv. Earth Sci.*, 21, 1260–1267, X–XI, 2006. 10278
- Miehe, G., Miehe, S., Bach, K., Nölling, J., Hanspach, J., Reudenbach, C., Kaiser, K., Wesche, K., Mosbrugger, V., Yang, Y., and Ma, Y.: Plant communities of central Tibetan pastures in the Alpine Steppe/Kobresia pygmaea ecotone, *J. Arid Environ.*, 75, 711–723, doi:10.1016/j.jaridenv.2011.03.001, 2011. 10277
- 15 Oberhuber, J. M., Herzog, M., Graf, H., and Schwanke, K.: Volcanic plume simulation on large scales, *J. Volcanol. Geoth. Res.*, 87, 29–53, doi:10.1016/S0377-0273(98)00099-7, 1998. 10280
- 20 Panin, G. N., Tetzlaff, G., and Raabe, A.: Inhomogeneity of the Land Surface and Problems in the Parameterization of Surface Fluxes in Natural Conditions, *Theor. Appl. Climatol.*, 60, 163–178, doi:10.1007/s007040050041, 1998. 10286
- Panin, G. N., Nasonov, A. E., and Foken, T.: Evaporation and heat exchange of a body of water with the atmosphere in a shallow zone, *Izvestiya, Atmos. Ocean. Phys.*, 42, 337–352, doi:10.1134/S0001433806030078, 2006. 10288, 10307
- 25 Ruppert, J., Thomas, C., and Foken, T.: Scalar Similarity for Relaxed Eddy Accumulation Methods, *Bound.-Lay. Meteorol.*, 120, 39–63, doi:10.1007/s10546-005-9043-3, 2006. 10290
- Sellers, P. J., Mintz, Y., Sud, Y. C., and Dalcher, A.: A Simple Biosphere Model (SIB) for Use within General Circulation Models, *J. Atmos. Sci.*, 43, 505–531, 1986. 10281
- 30 Su, Z., Wen, J., Dente, L., van der Velde, R., Wang, L., Ma, Y., Yang, K., and Hu, Z.: The Tibetan Plateau observatory of plateau scale soil moisture and soil temperature (Tibet-Obs) for quantifying uncertainties in coarse resolution satellite and model products, *Hydrol. Earth Syst. Sci.*, 15, 2303–2316, doi:10.5194/hess-15-2303-2011, 2011. 10277

10298

- Twine, T. E., Kustas, W. P., Norman, J. M., Cook, D. R., Houser, P. R., Meyers, T. P., Prueger, J. H., Starks, P. J., and Wesely, M. L.: Correcting eddy-covariance flux underestimates over a grassland, *Agric. For. Meteorol.*, 103, 279–300, doi:10.1016/S0168-1923(00)00123-4, 2000. 10286
- 5 van Heerwaarden, C. C., de Arellano, J. V., Moene, A. F., and Holtslag, A. A. M.: Interactions between dry-air entrainment, surface evaporation and convective boundary-layer development, *Q. J. Roy. Meteorol. Soc.*, 135, 1277–1291, doi:10.1002/qj.431, 2009. 10276
- Xue, Y., Zeng, F. J., and Schlosser, C. A.: SSiB and its sensitivity to soil properties – a case study using HAPEX-Mobilhy data, *Glob. Planet. Change*, 13, 183–194, doi:10.1016/0921-8181(95)00045-3, 1996. 10281
- 10 Yang, K., Koike, T., and Yang, D.: Surface Flux Parameterization in the Tibetan Plateau, *Bound.-Lay. Meteorol.*, 106, 245–262, doi:10.1023/A:1021152407334, 2003. 10277
- Yang, K., Chen, Y.-Y., and Qin, J.: Some practical notes on the land surface modeling in the Tibetan Plateau, *Hydrol. Earth Syst. Sci.*, 13, 687–701, doi:10.5194/hess-13-687-2009, 2009. 10277
- 15 Yee, S. Y. K.: The force-restore method revisited, *Bound.-Lay. Meteorol.*, 43, 85–90, doi:10.1007/BF00153970, 1988. 10282
- Zhou, D., Eigenmann, R., Babel, W., Foken, T., and Ma, Y.: The study of near-ground free convection conditions at Nam Co station on the Tibetan Plateau, *Theor. Appl. Climatol.*, 105, 217–228, doi:10.1007/s00704-010-0393-5, 2011. 10279, 10285
- 20

10299

**Table 1.** Description of the two sites near Nam Co lake used in this work.

Site	UBT	ITP
Coordinates	30°46.50' N 90°57.61' E	30°46.44' N 90°57.72' E
Soil	sandy-loamy	sandy
Porosity	0.63	0.393
Field Capacity	0.184	0.05
Wilting Point	0.115	0.02
Heat capacity ( $c_p$ ) [ $\text{Jm}^{-3}\text{K}^{-1}$ ]	$2.5 \times 10^6$	$2.2 \times 10^6$
Thermal Conductivity [ $\text{Wm}^{-1}\text{K}^{-1}$ ]	0.53	0.20
Surface Albedo ( $\alpha$ )	0.2	0.2
Surface Emissivity ( $\epsilon$ )	0.97	0.97
Vegetated Fraction	0.9	0.6
LAI [ $\text{m}^2\text{m}^{-2}$ ]	0.9	0.6
Vegetation height [m]	0.07	0.15

10300

**Table 2.** Initial soil temperatures used in study ( $\bar{T}_2$  and  $\bar{T}_1$  are estimated from the respective base and top temperatures of the layer according to a quadratic temperature profile), change of layer 1 mean temperature ( $\Delta\bar{T}_1$ ) over the modified Hybrid run, soil moisture content of layer 1 at beginning of the modified model run ( $\theta_{1,obs}$ ) and at the end of the simulation ( $\theta_{1,end}$ ). The values in parenthesis are expressed as  $\theta_1/FC$  [-].

Site	Date	$\bar{T}_2$ [°C]	$T_{1,base}$ [°C]	$\bar{T}_1$ [°C]	$T_0$ [°C]	$\Delta\bar{T}_1$ [°C]	$\theta_{1,obs}$ [%]	$\theta_{1,end}$ [%]
UBT	10 July	3.9	11.8	10.9	9.3	-1.6	26.9 (1.47)	41.1(2.24)
	27 July	4.5	13.4	12.5	10.6	-1.6	20.8 (1.14)	17.0 (0.92)
	05 August	4.8	14.4	13.4	11.2	-3.0	26.9 (1.47)	19.1 (1.04)
	06 August	4.75	14.3	12.8	9.8	-1.4	25.4 (1.39)	34.0 (1.85)
ITP	10 July	5.4	16.2	13.2	7.2	-1.2	6.0 (1.1)	25.1 (5.02)
	27 July	7.2	21.6	17.8	10.2	-1.7	3.0 (0.6)	1.6 (0.32)
	05 August	5.7	17.1	11.1	-0.8	0.2	11.0 (2.2)	4.3 (0.86)
	06 August	5.6	16.8	11.6	1.1	1.9	9.0 (1.8)	3.7 (0.73)

10301

**Table 3.** Root mean square deviation (RMSD) between the modelled quantities of the original and modified Hybrid and reference values. The reference quantities used are either measured by EC and corrected for energy balance closure (EC,EBC) or modelled with SEWAB for fluxes or taken from longwave outgoing radiation for  $T_0$ . The values in parenthesis ( $N$ ) correspond to the number of elements used for calculation of RMSD and  $R^2(l=0)$  in Fig. 7.

Site	Date	Run	RMSD				
			$Q_E$ EC,EBC [Wm <sup>-2</sup> ]	$Q_H$ [Wm <sup>-2</sup> ]	$Q_E$ SEWAB [Wm <sup>-2</sup> ]	$Q_H$ [Wm <sup>-2</sup> ]	$T_0$ [°C]
UBT	10 July	orig	318	117 (8)	94	74 (94)	4.3 (139)
	27 July		97	58 (19)	60	59 (139)	4.5 (143)
	05 August		168	139 (11)	90	64 (110)	4.3 (143)
	06 August		159	84 (52)	87	71 (128)	3.7 (143)
ITP	10 July	orig	182	93 (25)	97	69 (143)	3.7 (143)
	27 July		43	64 (72)	58	75 (143)	3.8 (143)
	05 August		224	103 (64)	179	68 (143)	8.3 (143)
	06 August		118	80 (52)	130	119 (143)	5.1 (143)
UBT	10 July	mod	214	43 (8)	51	36 (94)	2.3 (139)
	27 July		79	44 (19)	32	28 (139)	2.9 (143)
	05 August		93	62 (11)	36	26 (110)	3.4 (143)
	06 August		78	57 (52)	39	32 (128)	3.2 (143)
ITP	10 July	mod	74	73 (25)	42	32 (143)	1.6 (143)
	27 July		42	58 (72)	55	36 (143)	2.6 (143)
	05 August		44	80 (64)	64	30 (143)	2.6 (143)
	06 August		68	82 (52)	113	77 (143)	3.5 (143)
UBT	all	orig	170	92 (90)	83	67 (471)	4.2 (568)
		mod	100	54 (90)	39	31 (471)	3.0 (568)
ITP	all	orig	152	84 (213)	125	86 (572)	5.6 (572)
		mod	54	73 (213)	74	48 (572)	2.7 (572)

10302

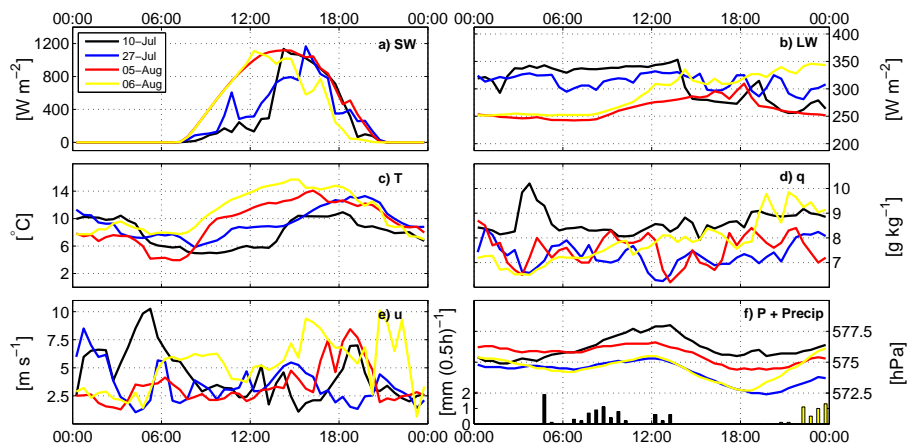


**Fig. 1.** Forcing data measured at UBT used for model runs: **(a)** downward shortwave radiation ( $SW$  [ $W m^{-2}$ ]); **b)** downward longwave radiation ( $LW$  [ $W m^{-2}$ ]); **(c)** air temperature ( $T$  [ $^{\circ}C$ ]); **(d)** water vapour mixing ratio ( $q$  [ $g kg^{-1}$ ]); **(e)** wind speed ( $U$  [ $ms^{-1}$ ]); **(f)** surface pressure ( $P$  [hPa]) and precipitation [ $mm(0.5h)^{-1}$ ]) Height c–e is 3 m.

10303

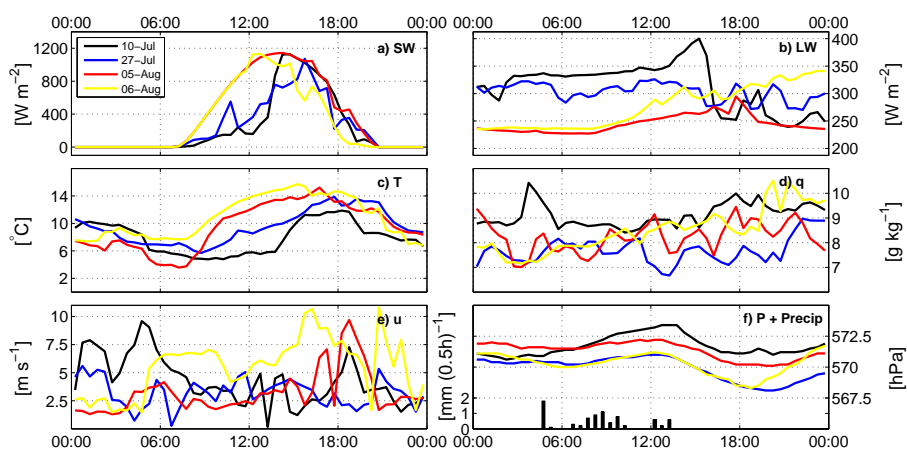


**Fig. 2.** Same as Fig. 1, but with forcing data measured at ITP.

10304

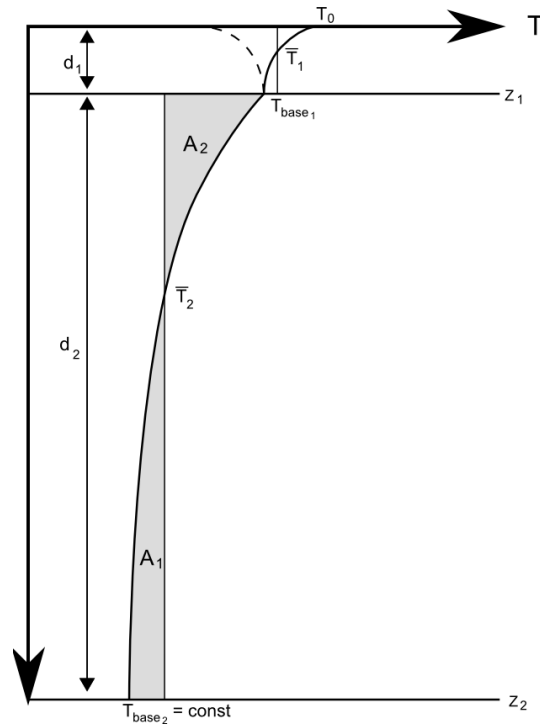


**Fig. 3.** Conceptual drawing of the assumed quadratic subgrid soil temperature profile and the associated parameters. In order to derive  $\bar{T}_1$  and  $\bar{T}_2$  geometrically the areas  $A_1$  and  $A_2$  must be equal.

10305

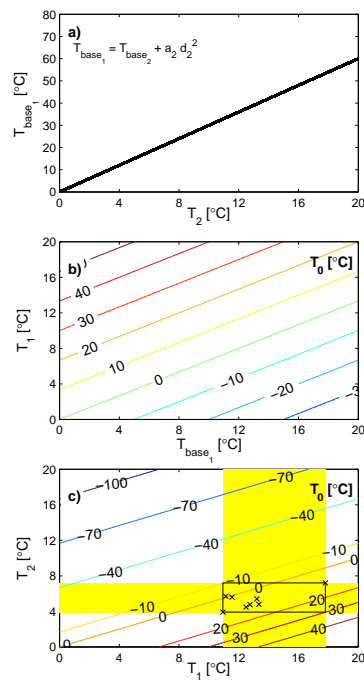


**Fig. 4.** Dependency of soil temperature parameters: **(a)** relationship between mean temperature of layer 2 ( $\bar{T}_2$ ) and bottom temperature of layer 1 ( $T_{base1}$ ) –  $a_2$  is calculated according to Eq. (4); **(b)** surface temperature ( $T_0$ ) contour plot as function of  $T_{base1}$  and layer 1 mean temperature ( $\bar{T}_1$ ) and **(c)** contours of ( $T_0$ ) as function of  $\bar{T}_2$  and  $\bar{T}_1$ . The black rectangle at the intersection of the layer temperature ranges (yellow) indicates the theoretical parameter space given by the temperature values used in this study and the black crosses mark the actual configurations.

10306



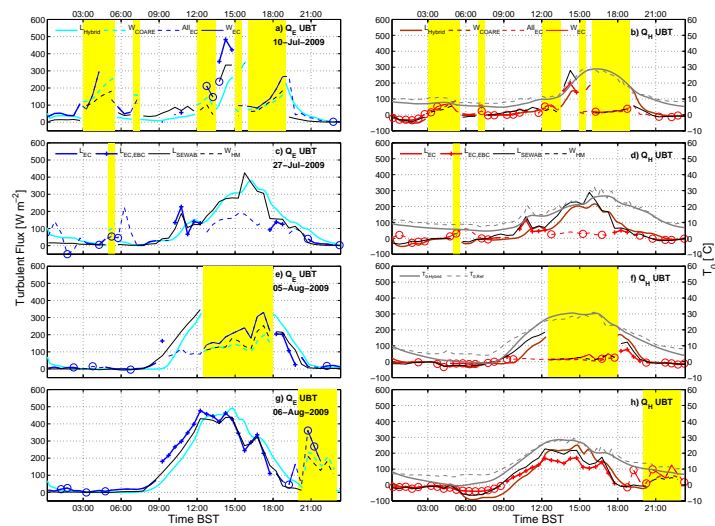


**Fig. 5.** Model results for the modified Hybrid at UBT for 10 July 2009 (a–b), 27 July 2009 (c–d), 5 August 2009 (e–f) and 6 August 2009 (g–h). Left column: latent heat flux ( $Q_E$ ); right column: sensible heat flux ( $Q_H$ ) and surface temperature  $T_s$  [ $^{\circ}\text{C}$ ].  $L$  and  $W$  refer to “land” and “water” as origin of the fluxes.  $All$  is the complete available time series. The subscript *Hybrid* refers to fluxes from Hybrid and *COARE* are fluxes from the lake derived by TOGA-COARE whereas *SEWAB* is a SVAT model and *HM* refers to a hydrodynamic multi-layer lake model after Foken (1984) and Panin et al. (2006). *EC* and *EC,EBC* refer to measurements by eddy covariance method where in the latter the energy balance has been closed by distributing the residual according to Bowen-ratio (this requires good data quality and fluxes and can only be done for fluxes that are attributed to land). The circles indicate poor data quality of the EC system according to Foken et al. (2004). Yellow shading indicates times where the flux footprint of UBT was over the lake.

10307

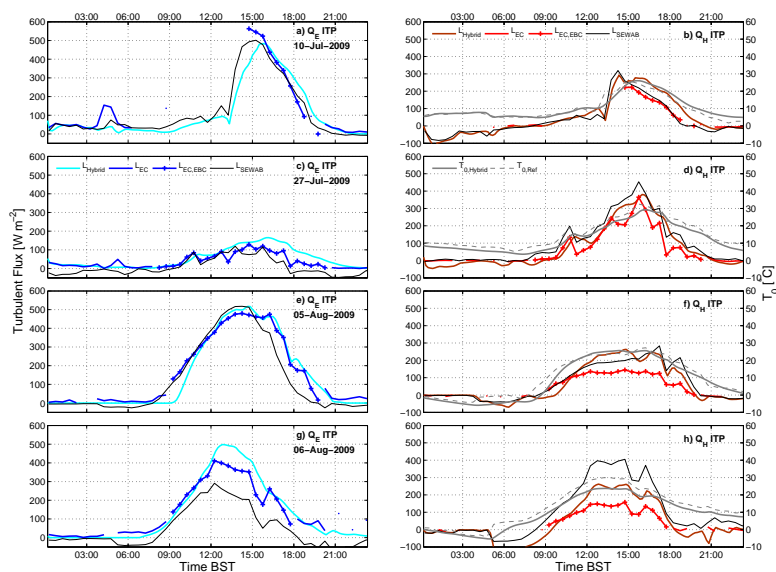


**Fig. 6.** Same as Fig. 5, but for ITP. There are no contributions from the lake.

10308

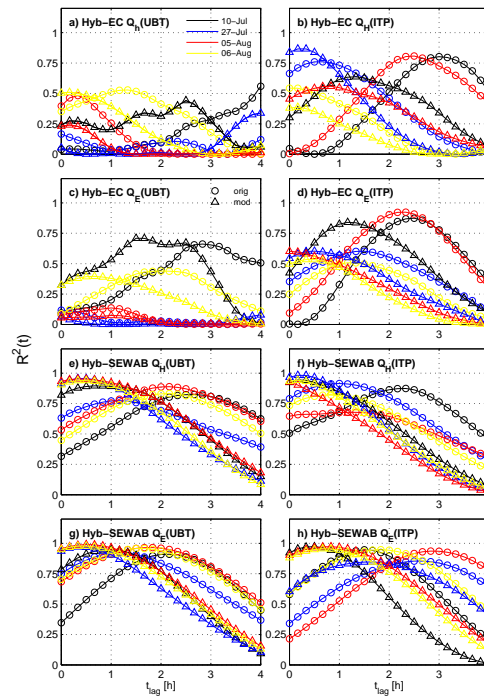


**Fig. 7.** Correlation of simulated fluxes against flux reference shifted by  $t_{lag}$  as multiples of 10 minutes (Cross Correlation –  $R^2(t)$ ) for each of the four days simulated and for the original and modified Hybrid. The maximum number of elements used in the calculation of  $R^2$  for each curve can be taken from Table 3.